IDENTIFICATION OF CONTINUOUS-TIME NOISE MODELS

R. Pintelon[(1)], J. Schoukens[(1)], Y. Rolain[(1)], B. Cauberghe[(2)], E. Parloo[(2)], and P. Guillaume[(2)]

Vrije Universiteit Brussel, Dept. [(1)]ELEC, [(2)]WERK, Pleinlaan 2, 1050 Brussel, Belgium

Abstract: Current methods identify the physical parameters of continuous-time ARMA(X) processes via discrete-time approximations. Based on a frequency domain maximum likelihood estimator described in Ljung (1999), this paper proposes an exact continuous-time noise modeling approach. The theory is illustrated on real measurement examples.

Keywords**:** system identification, frequency-domain method, continuous-time systems, noise characterization, open loop, parameter estimation.

1. INTRODUCTION

The goal of operational modal analysis is to estimate the resonance frequencies and damping ratios of mechanical structures (bridge, air plane, building …) from their response to non-measurable external forces induced by e.g. the wind, earth quakes, traffic, turbulence … The classical approach for identifying these physical parameters consists in straightforward discrete-time ARMA modeling of the true continuous-time process from discrete-time data (Peeters and De Roeck, 2001). Refined discrete-time approximations are proposed in Walhlberg *et al.* (1993), Söderström *et al.* (1997), and Fan *et al.* (1999). In this paper we model the continuous-time noise processes using the frequency domain Box-Jenkins framework developed in Ljung (1999) for data collected in open loop. The advantages of this modeling approach are (i) it is exact for a realistic class of continuous-time noise processes, (ii) it can handle time domain as well as frequency domain data.

The main contributions of this paper are the following. (i) A theoretical justification is given for modeling the noise at the sampling instances as filtered continuous-time band-limited white noise. As such the continuous-time Box-Jenkins (BJ) model can be used for physical modeling of continuous-time stochastic processes. (ii) It is shown that the maximum likelihood (ML) cost function described in Ljung (1999) can be reduced to a quadratic-like form. As a consequence classical Newton-Gauss based iterative schemes can still be used for calculating the ML estimates. (iii) The usefulness and feasibility of the proposed continuous-time modeling approach is illustrated on two real life problems: operational modal analysis of a bridge, and flight flutter testing.

This work is supported by the Fund for Scientific Research Flanders; the Belgian Government (IUAPV/22); and the Flemish Community (GOA-IMMI).

2. THE NOISE MODEL

The response $n(t)$ of a lumped time-invariant continuous-time system to a second order continuous-time stationary stochastic process $e_c(t)$ can be written as

$$n(t) = H(p)e_c(t) \tag{1}$$

with p the derivative operator ($px(t) = dx(t)/dt$), and $H(p)$ a rational form of p (Åström, 1970).

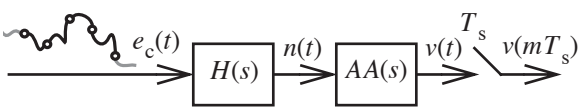

Fig. 1. Band-limited noise and measurement assumption. T_s is the sample period and $AA(s)$ the anti-alias filter.

Without any loss of generality we will assume that $e_c(t)$ has zero mean. The fact that the values of $e_c(t)$ at different times are correlated complicates the handling of $n(t)$ in identification algorithms. Therefore, it is tempting to study (1) for continuous-time white noise $e_c(t)$. However, since continuous-time white noise has infinite variance, this leads to the mathematical difficulty of treating stochastic differential equations (Åström, 1970). A way to avoid the difficulty of handling correlated driving noise sources $e_c(t)$ or stochastic differential equations is to use the concept of band-limited (BL) white noise (Åström, 1970). In the sequel of the section it is shown that in a BL-measurement set up (Pintelon and Schoukens, 2001) (1) can be approximated very well at the sampling instances by filtered continuous-time band-limited white noise.

Consider the measurement set up shown in Fig. 1.

Assumption 1 (Band-limited)
(a) BL-white noise: the power spectral density $S_{e_c}(f)$ (Fourier transform of the auto-correlation of $e_c(t)$) is constant for $|f| < f_B$ and zero elsewhere, where $f_B \geq f_s/2$, with $f_s = 1/T_s$ the sampling frequency.
(b) BL-set up: the anti-alias filter $AA(s)$ in the measurement set up is perfect $AA(j2\pi f) = 1$ for $|f| < f_s/2$ and zero elsewhere. □

Theorem 1: Under Assumption 1 the band-limited observation $v(t)$ of $n(t)$ (1) is exactly described by following continuous-time noise process

$$v(t) = H(p)e(t) \tag{2}$$

with $H = H_c$, $e(t)$ continuous-time band-limited white noise. At the sampling instances $t = nT_s$, $e(t)$ is discrete-time white noise with zero mean and variance σ^2.

Proof: Using Assumption 1, the power spectral density $S_v(f)$ of $v(t)$ equals

$$\begin{aligned} S_v(f) &= |H(j2\pi f)|^2 |AA(j2\pi f)|^2 S_{e_c}(f) \\ &= |H(j2\pi f)|^2 S_e(f) \end{aligned} \tag{3}$$

where $S_e(f) = |AA(j2\pi f)|^2 S_{e_c}(f)$ is the power spectral density of band-limited zero mean white noise $e(t)$ with bandwidth $f_s/2$. Defining $S_e(f) = \sigma^2/f_s$ for $|f| < f_s/2$, the auto-correlation $R_e(\tau)$ of $e(t)$ equals

$$R_e(\tau) = F^{-1}\{S_e(f)\} = \sigma^2 \mathrm{sinc}(\pi f_s \tau) \tag{4}$$

with $F^{-1}\{\}$ the inverse Fourier transform, and $R_e(0) = \mathrm{var}(e(t)) = \sigma^2$. Since $R_e(nT_s) = 0$ for $n \neq 0$, it follows that $e(t)$ is uncorrelated at the sampling instances $t = nT_s$. □

Note that the proof of Theorem 1 still holds when the BL-signal condition in Assumption 1 ($S_{e_c}(f) = 0$ for $|f| \geq f_B$) is relaxed to

$$S_{e_c}(f) = o(f^{-1}) \text{ for } |f| \geq f_B, \tag{5}$$

which is the weakest decay giving a finite variance $\mathrm{var}(e_c(t)) = \int_{-\infty}^{+\infty} S_{e_c}(f)df < \infty$. If the anti-alias filter $AA(s)$ is not ideal, then (2) is an approximation of BL-observations of (1) at the sampling instances.

Using the BL assumption/CT model (2), the relationship between the discrete Fourier transform (DFT) $V(k)$ of the measured samples $v(nT_s)$, $n = 0, 1, \ldots, N-1$, and the DFT $E(k)$ of the driving white noise samples $e(nT_s)$, $n = 0, 1, \ldots, N-1$, is given by

$$V(k) = H(s_k)E(k) + T_H(s_k) \tag{6}$$

where $s_k = j2\pi k f_s/N$ and

$$X(k) = N^{-1/2} \sum_{n=0}^{N-1} x(nT_s) z_k^{-n} \tag{7}$$

the DFT of $x(nT_s)$ with $X = V, E$ and $x = v, e$ (Pintelon and Schoukens, 2001). The noise transfer function H and the noise transient term T_H are rational functions of the Laplace variable s

$$\begin{aligned} H(s) &= \frac{C(s)}{D(s)} = \left[\sum_{r=0}^{n_c} c_r s^r\right] \Big/ \left[\sum_{r=0}^{n_d} d_r s^r\right] \\ T_H(s) &= \frac{I_H(s)}{D(s)} = \left[\sum_{r=0}^{n_{i_h}} i_{h_r} s^r\right] \Big/ \left[\sum_{r=0}^{n_d} d_r s^r\right] \end{aligned}, \tag{8}$$

where $n_{i_h} > \max(n_c, n_d) - 1$. The numerator coefficients i_{h_r} of T_H depend on the initial and final conditions of the experiment and decrease as an $O(N^{-1/2})$ as $N \to \infty$. Hence, for N sufficiently large, the transient term T_H in (6) can be neglected w.r.t. $H(\Omega_k)E(k)$ (Pintelon and Schoukens, 2001).

The DFT $E(k)$ of the driving white noise source $e(nT_s)$ has the following properties. Since $e(nT_s)$ is zero mean white (uncorrelated over n) noise, it

follows that $E(k)$ (7) is zero mean white (uncorrelated over k) noise with $\mathrm{var}(E(k)) = \mathrm{var}(e(t)) = \sigma^2$ and $\mathcal{E}\{E^2(k)\} = 0$ (= circular complex distributed) (Pintelon and Schoukens, 2001). If $e(nT_s)$ is normally distributed, then $E(k)$ is circular complex normally distributed. If $e(nT_s)$ is independent and identically distributed with existing moments of any order, then $E(k)$ is asymptotically ($N \to \infty$) independent, circular complex normally distributed (see Pintelon and Schoukens, 2001, Lemma 14.24).

All these properties motivate the following noise assumptions in the frequency domain.

Assumption 2 (Noise model)
The observed frequency domain noise $V(k)$ can be written as

$$V(k) = H(s_k)E(k) \tag{9}$$

where $H(s)$ is defined in (8). $E(k)$ is independent (over k), circular complex ($\mathcal{E}\{E^2(k)\} = 0$) normally distributed noise, with zero mean, and variance $\lambda = \mathrm{var}(E(k)) = \mathcal{E}\{|E(k)|^2\}$. □

3. PLANT MODEL

The BL-assumption (Assumption 1.b) on the measurement set up, leads in a natural way to a CT-representation of the plant

$$y(t) = G(p)u(t) \tag{10}$$

The input $U(k)$ and output $Y(k)$ DFT spectra are then related by

$$Y(k) = G(s_k)U(k) + T_G(s_k) \tag{11}$$

where the plant G and the plant transient T_G transfer functions are rational forms of the Laplace variable s

$$\begin{aligned} G(s) &= \frac{B(s)}{A(s)} = \left[\sum_{r=0}^{n_b} b_r s^r\right] \Big/ \left[\sum_{r=0}^{n_a} a_r s^r\right] \\ T_G(s) &= \frac{I_G(s)}{A(s)} = \left[\sum_{r=0}^{n_{i_g}} i_{g_r} s^r\right] \Big/ \left[\sum_{r=0}^{n_a} a_r s^r\right] \end{aligned}, \tag{12}$$

with $n_{i_g} > \max(n_a, n_b) - 1$ (Pintelon and Schoukens, 2001). Similarly to (6), the numerator coefficients i_{g_r} of T_G decrease as an $O(N^{-1/2})$ and, hence, for N sufficiently large, the transient term T_G in (11) can be neglected w.r.t. $G(s_k)U(k)$. It motivates the following plant model assumption in the frequency domain.

Assumption 3 (Plant model)
The input $U(k)$ and output $Y(k)$ frequency domain data are related by

$$Y(k) = G(s_k)U(k) \tag{13}$$

where $G(s)$ is defined in (12). □

4. OPEN LOOP FRAMEWORK

The stochastic framework is set by the following assumption.

Assumption 4 (Open loop)
(a) The input and output are observed without errors.
(b) The observed output is the sum of the plant response to the input, and the process noise.
(c) The input is independent of the process noise.

Under Assumptions 2-4, the observed input and output frequency domain data are respectively related by

$$Y(k) = G(s_k)U(k) + H(s_k)E(k) \tag{14}$$

According to the particular parametrization of the plant (12) and noise (8) model one distinguishes different model structures, such as ARMA ($G = 0$), OE ($H = 1$), ARMAX ($D = A$), BJ, …

5. IDENTIFICATION OF THE PLANT AND NOISE MODEL PARAMETERS

5.1 Maximum likelihood cost function

Consider the parametric models $G(s, \theta)$ (12) and $H(s, \theta)$ (8), with $\theta = [a^T, b^T, c^T, d^T]^T$

$$a^T = [a_0, a_1, \ldots, a_{n_a}], \ldots, d^T = [d_0, \ldots, d_{n_d}] \tag{15}$$

and assume that the frequency domain data $U(k)$, $Y(k)$ is available at frequencies $k = 1, 2, \ldots, F$.

Theorem 2 (Log-likelihood function): Under Assumptions 2-4 the negative Gaussian log-likelihood function is, within a constant, given by

$$\sum_{k=1}^{F} \log\left(\lambda \left|H(s_k, \theta)\right|^2\right) + \frac{1}{\lambda}\sum_{k=1}^{F} \left|\varepsilon(s_k, \theta)\right|^2 \tag{16}$$

with $\lambda = \mathrm{var}(E(k))$, and ε the prediction error,

$$\varepsilon(s_k, \theta) = (Y(k) - G(s_k, \theta)U(k)) / H(s_k, \theta) \tag{17}$$

Table 1 Possible parameter constraints

Model structure	Constraints on θ
ARMA	$c_{n_c} = d_{n_d} = 1$
OE	$a_{n_a} = 1$
ARMAX	$a_{n_a} = c_{n_c} = 1$
Box-Jenkins (BJ)	$a_{n_a} = c_{n_c} = d_{n_d} = 1$

Proof: see Ljung (1999), p. 230. □

By eliminating λ, cost function (16) can be simplified to a quadratic function of the residuals.

Theorem 3 (Maximum likelihood cost function): Under the assumptions of Theorem 2 the Gaussian maximum likelihood (ML) cost function $V_F(\theta, Z)$ is given by

$$V_F(\theta, Z) = \frac{1}{F}\sum_{k=1}^{F} \left|\varepsilon(s_k, \theta) g_F(\theta)\right|^2$$
$$g_F(\theta) = \exp\left(\frac{1}{F}\sum_{k=1}^{F} \log H(s_k, \theta)\right) \quad , \qquad (18)$$

with $\varepsilon(s_k, \theta)$ defined in (17).

Proof: Calculating the derivative of (16) w.r.t. λ gives

$$\lambda(\theta) = \frac{1}{F}\sum_{k=1}^{F} \left|\varepsilon(s_k, \theta)\right|^2 \qquad (19)$$

Eliminating λ in (16) using (19) and taking the exponential function gives (18) within a θ-independent constant. □

As a result the minimizer of (18) can be calculated in a numerical stable way via the iterative Newton-Gauss and Levenberg-Marquardt methods.

5.2 Maximum likelihood estimator

The parametric models $G(s, \theta)$ (12) and $H(s, \theta)$ (8) are overparametrized. Indeed, replacing e.g. in a Box-Jenkins model parameters a, b, c, d by $\gamma_1 a$, $\gamma_1 b$, $\gamma_2 c$, $\gamma_2 d$ respectively, leaves the plant and noise models unchanged. Further, the fact that $E(k)$ in (14) is not observed, and that the term $H(s_k, \theta)E(k)$ remains the same when multiplying $H(s_k, \theta)$ and dividing $E(k)$ by the same non-zero real number γ, imposes an additional constraint on the parameters of $H(s, \theta)$. Hence, according to the particular model structure, one (OE), two (ARMA, ARMAX), or three (BJ) parameter constraints are needed (see Table 1). Since the cost function $V_F(\theta, Z)$ (18) contains exactly the same parameter ambiguities as $G(s, \theta)$ (12), $H(s, \theta)$ (8), and $H(s_k, \theta)E(k)$ in (14), the estimated models $G(s, \hat{\theta})$ and $\hat{\lambda}^{1/2}H(s, \hat{\theta})$, with $\hat{\theta}$ the minimizer of (18) and $\hat{\lambda} = \lambda(\theta)$ (19), are independent of the particular parameter constraint(s) chosen (Pintelon and Schoukens, 2001).

Cost function (18), subject to the constraints of Table 1, still contains another parameter ambiguity. Indeed, let $\alpha + j\beta$ be a zero of $H(s, \theta)$ or a pole of $H(s, \theta)$ not in common with $G(s, \theta)$, then with some abuse of notation the cost function (18) has the property

$$V_F(-\alpha + j\beta, Z) = V_F(\alpha + j\beta, Z) \qquad (20)$$

It shows that no distinction can be made between noise models which only differ in poles and/or zeros that are mirrored w.r.t. the $j\omega$-axis, and that $V_F(\theta, Z)$ contains at least as many global minima as possible mirrored noise pole/zero patterns. As a practical result one should not stabilize the zeroes (and poles) of the noise model during the minimization of (18). The identifiability problem is avoided by restricting the allowable poles/zeros positions of the noise model to the stable region of the s-domain.

Assumption 5 (Constraint noise model)
$H^{-1}(s, \theta)$ is a stable transfer function. The poles of $H(s, \theta)$ that are not in common with $G(s, \theta)$ are stable. □

These results are summarized in the following theorem.

Theorem 4 (ML estimator): Under Assumptions 2-5 the maximum likelihood (ML) estimator $\hat{\theta}(Z)$ of the plant and noise model parameters minimizes (18) subject to the constraints in Table 1.

Theorem 4 describes the ML estimator starting from frequency domain data $U(k)$, $Y(k)$ (Assumptions 2-4) described by model (14). If the raw data are time domain signals then (14) and (18) are asymptotically (time domain samples $N \to \infty$) valid. To improve the finite sample behaviour of the estimate $\hat{\theta}(Z)$, model (14) is replaced by the sum of (6) and (11)

$$Y(k) = G(s_k)U(k) + H(s_k)E(k) + T_G(s_k) + T_H(s_k) \qquad (21)$$

This results in the same cost function (18) where the prediction error $\varepsilon(s_k, \theta)$ is replaced by

$$\varepsilon(s_k, \theta) = H^{-1}(s_k, \theta)[Y(k) - G(s_k, \theta)U(k) - T_G(s_k, \theta) - T_H(s_k, \theta)] \qquad (22)$$

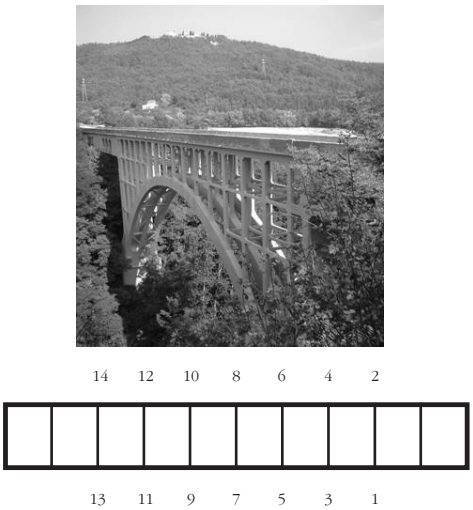

Fig. 2. Villa Paso bridge. Top: picture bridge. Bottom: schematic top view with numbered test points.

6. APPLICATIONS

In both examples the input/output signals are lowpass filtered before sampling.

6.1 Villa Paso bridge

The Villa Paso arch bridge shown in Fig. 2 is excited by the traffic in its vertical direction and by the wind mainly in its horizontal direction. These excitations cannot be measured and are assumed to be white in the frequency band of interest (= operational modal analysis). Acceleration measurements have been performed on the deck of the bridge at fourteen test points, both in horizontal and vertical direction (see Fig. 2). All signals are measured simultaneously during about 14 min. at the sampling rate $f_s = 400\,\text{Hz}$, giving $N = 337700$ data points per measurement channel. Only the measurements in the horizontal direction at test points one and six are handled here. This data is modelled in the frequency band [1.18 Hz, 4.14 Hz] (DFT lines $k = 999, 1000, \ldots, 3499 \Rightarrow F = 2501$) with a CT-ARMA model structure of order 8/8 ($n_c = n_d = 8$, and $n_{i_h} = 11$). Fig. 3 validates the identified noise model $\lambda^{1/2}(\hat{\theta})\left|H(s_k, \hat{\theta})\right|$ with the measured noise DFT spectrum $\hat{V}(k)$

$$\hat{V}(k) = Y(k) - T_H(s_k, \hat{\theta}) \qquad (23)$$

The zero patterns of the noise models differ because they depend on the location of the test point on the bridge. Table 2 gives the estimated resonance frequencies and damping ratios. It can be seen that the differences between the two results are much smaller than the standard deviation of the estimates. This can be explained as follows: since the measurements at the two test points are done simultaneously, the observed signals stem from the same realisation of the driving white noise source (the wind) and, hence, the two estimates are not independent of each other.

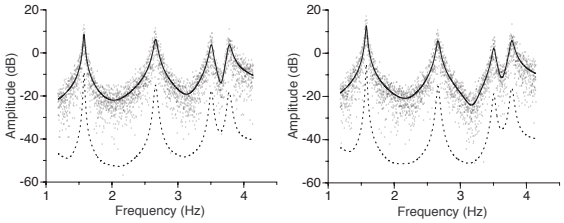

Fig. 3. Validation of the identified CT ARMA model (order 8/8) of the Villa Paso bridge at test points one (left) and six (right). Dots: measured noise spectrum $\hat{V}(k)$. Solid line: noise model times standard deviation driving white noise source. Dashed line: standard deviation model.

Table 2 Estimated resonance frequencies f_0 and damping ratios ζ of the Villa Paso bridge

	test point 1	test point 6
$f_{0,1} \pm \text{std}(f_{0,1})$ (Hz)	1.5759 ± 0.0016	1.5763 ± 0.0016
$\zeta_1 \pm \text{std}(\zeta_1)$ (%)	0.73 ± 0.10	0.74 ± 0.10
$f_{0,2} \pm \text{std}(f_{0,2})$ (Hz)	2.6623 ± 0.0025	2.6622 ± 0.0025
$\zeta_2 \pm \text{std}(\zeta_2)$ (%)	0.99 ± 0.10	0.96 ± 0.09
$f_{0,3} \pm \text{std}(f_{0,3})$ (Hz)	3.5068 ± 0.0030	3.5067 ± 0.0031
$\zeta_3 \pm \text{std}(\zeta_3)$ (%)	0.80 ± 0.08	0.78 ± 0.09
$f_{0,4} \pm \text{std}(f_{0,4})$ (Hz)	3.7756 ± 0.0034	3.7759 ± 0.0033
$\zeta_4 \pm \text{std}(\zeta_4)$ (%)	0.89 ± 0.09	0.88 ± 0.09

6.2 Flight flutter testing

To excite the air plane during flight, a perturbation signal is injected in the control loop of the flap mechanism at the tip side of the right wing. The angle perturbation of the flap is used as a measure of the applied force, and the acceleration is measured at the tip of the left wing. Beside the applied perturbation, the air plane is also excited during flight by the natural turbulence. The resulting turbulent forces acting on the air plane cannot be measured and are assumed to be white in the frequency band of interest. The input/output signals are measured during about 109 s at the sampling rate $f_s = 300\,\text{Hz}$, giving $N = 32768$ data points per channel. Fig. 4 shows the force to acceleration frequency response function (FRF) in the band $[4.70\,\text{Hz}, 16.40\,\text{Hz}]$ (DTF lines $k = 513, 514, \ldots, 1791 \Rightarrow F = 1279$). Since it is not known beforehand whether the natural turbulence excites the same modes as the applied excitation, the

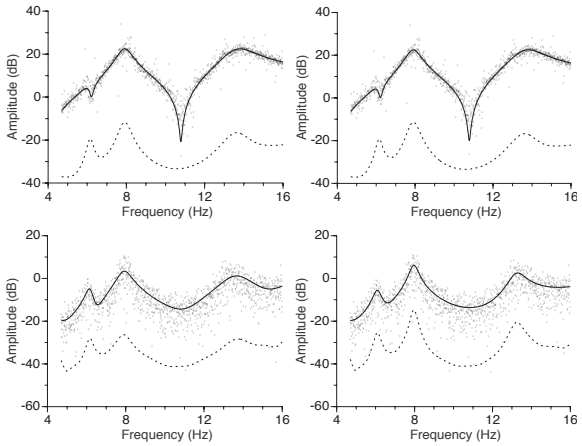

Fig. 4. Validation of the identified CT models of the flight flutter test. Top row: validation with the measured FRF $\hat{G}(j\omega_k)$. Bottom row: validation with the output residual $\hat{V}(k)$. Left column: ARMAX model. Right Column: BJ model. Dots: respectively measured FRF and output residual. Solid line: respectively estimated plant model and noise model times standard deviation driving white noise source. Dashed line: standard deviation estimated models.

data is modelled using a CT-BJ and a CT-ARMAX model structure. It turns out that a CT-BJ model of order $n_a = 6$, $n_b = 8$, $n_{i_g} = 2$, $n_c = 10$, $n_d = 6$, $n_{i_h} = 13$, and a CT ARMAX model of order $n_a = 6$, $n_b = 8$, $n_c = 10$, $n_{i_g} + n_{i_h} = 13$ explain the data very well (see Fig. 4). The FRF $\hat{G}(j\omega_k)$, and the output residual $\hat{V}(k)$ in Fig. 4 are calculated using

$$\begin{aligned} \hat{G}(j\omega_k) &= (Y(k) - T_G(s_k, \hat{\theta}) - T_H(\Omega_k, \hat{\theta}))/U(k) \\ \hat{V}(k) &= Y(k) - G(s_k, \hat{\theta})U(k) - T_G(s_k, \hat{\theta}) - T_H(s_k, \hat{\theta}) \end{aligned} \quad (24)$$

From Table 3 it can be seen that only the first pole of the BJ noise model coincides within its uncertainty with the first pole of the BJ plant model. For the air plane manufacturer it is important to know whether the air plane has five (BJ model) or three (ARMAX model) different resonance frequencies in the band $[4.70 \text{ Hz}, 16.40 \text{ Hz}]$. Although the ML cost function $V_F(\hat{\theta}, Z)$ (18) is the smallest for the BJ model structure (BJ: 0.202, ARMAX: 0.207), the minimum description length (MDL) criterion (Ljung, 1999),

$$V_F(\hat{\theta}, Z)e^{p(n_\theta, F)} \quad (25)$$

with $p(n_\theta, F) = n_\theta \log(F)/F$ and n_θ the number of free model parameters, selects the ARMAX model structure (BJ: 0.264, ARMAX: 0.257). However, since the differences between the criteria are small, more data are needed to give a decisive answer.

Table 3 Estimated resonance frequencies f_0 and damping ratios ζ of the flight flutter test

	ARMAX	BJ plant model	BJ noise model
$f_{0,1} \pm \text{std}(f_{0,1})$ (Hz)	6.171 ± 0.017	6.171 ± 0.018	6.101 ± 0.049
$\zeta_1 \pm \text{std}(\zeta_1)$ (%)	3.0 ± 0.3	3.0 ± 0.3	3.4 ± 0.8
$f_{0,2} \pm \text{std}(f_{0,2})$ (Hz)	7.9143 ± 0.0058	7.9040 ± 0.0060	7.962 ± 0.027
$\zeta_2 \pm \text{std}(\zeta_2)$ (%)	4.59 ± 0.07	4.61 ± 0.08	2.7 ± 0.3
$f_{0,3} \pm \text{std}(f_{0,3})$ (Hz)	13.651 ± 0.009	13.666 ± 0.008	13.232 ± 0.062
$\zeta_3 \pm \text{std}(\zeta_3)$ (%)	6.06 ± 0.06	6.02 ± 0.06	3.1 ± 0.5

7. CONCLUSION

Using the concept of band-limited (BL) white noise it has been shown that the noise observed in a BL measurement setup can be modelled exactly at the sampling instances as CT filtered BL white noise. The usefulness and feasibility of this modeling approach been demonstrated on two real measurement examples.

REFERENCES

Åström, K. J. (1970). *Introduction to Stochastic Control Theory.* Academic Press, New York (USA).

Fan, H., T. Söderström, M. Mossberg, B. Carlsson B and Y. J. Zou (1999). Estimation of continuous-time AR process parameters from discrete-time data. *IEEE Trans. Sign. Proc.,* **vol. 47**, no. 5, pp. 1232-1244.

Ljung, L. (1999). *System Identification: Theory for the User.* Prentice-Hall, Upper Saddle River, NJ.

Peeters, B. and G. De Roeck (2001). Stochastic system identification for operational modal analysis: a review. *ASME Trans. - Journ. of Dynamic Systems Meas. and Contr.,* **vol. 123**, no. 4, pp. 659-667.

Pintelon, R. and J. Schoukens (2001). *System Identification: a Frequency Domain Approach.* IEEE Press, Piscataway, NJ.

Söderström, T., H. Fan, B. Carlsson and S. Bigi (1997). Least squares parameter estimation of continuous-time ARX models from discrete-time data. *IEEE Trans. Autom. Contr.,* **vol. 4**, no. 5, pp. 659-673.

Wahlberg, B, L. Ljung and T. Söderström (1993). On sampling of continuous time stochastic processes. *Control-Theory and Advanced Technology,* **vol. 9**, no. 1, pp. 99-112.